Angle of Arrival Estimation Via Small IoT Devices: Miniaturized Arrays vs MIMO Antennas

Abel Zandamela, Alessandro Chiumento, Nicola Marchetti, and Adam Narbudowicz .

Abstract

This tutorial discusses the problem of Angle-of-Arrival (AoA) estimation from small Internet of Things (IoT) devices. It reviews the limitations and challenges of existing miniaturization strategies, which involve classical antenna arrays. As larger distance between antennas is typically needed for increased precision, the miniaturization without loss of accuracy is a significant problem. The article demonstrates that the use of electrically small antennas does not directly solve the problem, since smaller antennas may require increased distance to avoid coupling between elements. Therefore, this work proposes a new technique to perform AoA estimation in small platforms – a Multiple-Input Multiple-Output (MIMO) antenna. MIMO antennas are commonly used to increase the communication throughput, however few works have studied their usage for AoA estimation in line-of-sight environment. The proposed solution offers performance similar to state-of-the-art arrays, however at a substantially reduced size. Performance study is carried out to confirm and validate the proposed technique accuracy and miniaturization efficacy. Size reduction up to 75% compared to linear arrays is achieved with mean absolute errors smaller than 0.11°. The method also demonstrates a resolution of 5° with peak mean absolute error of 0.3° for two simultaneous impinging signals.

Angle of Arrival Estimation

Recent advances in digital electronics and wireless communications are contributing to the development of seamless Internet of Things (IoT) technologies [1]. IoT allows objects from daily life to exchange information with each other, sense their environment and remotely execute instructions. The plethora of IoT devices includes wireless sensors, smartphones, actuators, displays and many more.

An increasingly attractive feature of IoT is the capability to perform localization. A commonly used localization technique is Angle of Arrival (AoA) estimation, in which position information is retrieved based on the direction of impinging signals, typically on multiple receiving antennas [2], [3]. In the state-of-the-art, antenna arrays are employed, where AoA algorithms exploit the differential phase information from the outputs of multiple antennas [3]. This allows to determine the arriving signal's source direction. AoA technique differs from other localization methods such as received signal strength, time of flight, time difference of arrival, because it can provide high localization accuracy without requiring clock synchronization and fingerprinting, while also allowing for multiple signals separation [2], [3].

In this tutorial we propose a Multiple-Input Multiple-Output (MIMO) antenna to allow high precision AoA measurements while using compact IoT structures. The solution is comprised of collocated radiators, each exciting different orthogonal radiating modes. This principle provides sufficiently distinct phase variations for AoA estimation, while preserving good coupling characteristics. The achieved AoA estimation performance is comparable with 5-element linear and circular arrays, but with miniaturization up to 75% and 40%, respectively.

A. Zandamela, N. Marchetti and A. Narbudowicz are with CONNECT Centre, Trinity College Dublin, Dunlop Oriel House, 34 Westland Row, Dublin 2, Ireland (email: {zandamea, nicola.marchetti, narbudoa}@tcd.ie).

A. Narbudowicz is also with the Department of Telecommunications and Teleinformatics, Wroclaw University of Science and Technology, Wroclaw 50-370, Poland.

A. Chiumento is with the Department of Pervasive Systems, University of Twente, 7522 NB Enschede, The Netherlands (email: a.chiumento@utwente.nl)

Challenges in Performing AoA Estimation Using Compact IoT Devices

The main issue of AoA estimation with compact IoT systems stems from the fact that the accuracy of the measured AoA depends on the array size and the number of antennas involved. In other words, more accurate estimations are obtained with large arrays and increased number of antennas [3], [4]. However, the use of large array systems diverges from current technological trends, which require miniaturization due to physical size constraints. This is the case in many growing commercial applications such as localization systems using small unmanned aerial vehicles [4] and indoor position systems used for tracking and navigation [2]. Therefore, it is desirable to develop novel solutions to allow accurate AoA estimation while using compact devices [2]–[4].

The number of multiple signals that can be simultaneously detected by the array is limited to $N–1$ non-coherent signals, where N is the number of antennas involved [3]. Consequently, to separate multiple signals arriving from different directions, the number of array elements should also be increased. This exacerbates the problem of AoA estimation from compact devices, resulting in even more bulky systems.

Finally, the problem for compact devices is the mitigation of mutual coupling between array's elements. If antennas are placed close to each other, a fraction of the electromagnetic wave might couple from one element to the other, altering the radiation pattern, the gain, and ultimately deteriorating the overall performance [3], [5].

Recent Breakthroughs

As discussed above, reducing the inter-element spacing between the array elements to derive a compact AoA estimation system, results in increased mutual coupling in the antenna array. This problem has been extensively investigated in the literature, e.g. in a recent work by Pralon et. al [4]. Typically, decoupling and matching networks are used for mutual coupling mitigation. However, these solutions suffer from increased ohmic losses.

Single antenna solutions for AoA measurement have also been investigated, e.g. in [6] and [7]. While these works present a breakthrough by achieving low-power consumption and low-complexity, they generate multiple beams by sequentially connecting/disconnecting passive structures that surround the antenna. This allows to change radiation pattern within the duration of the signal to be estimated, which can correspond to sampling such signal using multiple antennas. Although this approach solves the issue of computational complexity, the size limitation remains, as surrounding passive structures require certain separation to produce the required variation between the radiation patterns. Moreover, due to the switching between different antenna configurations, additional time is needed in the AoA estimation. This can be a significant burden, especially when separating multiple moving sources, as they may change between consecutive antenna configurations. These approaches also have limited capability to localize multiple signals and are susceptible to manufacturing flaws.

In a recent study presented in [8], a systematic approach for designing platform-based high-frequency band AoA antenna arrays is proposed. The method relies on a systematic selection and excitation of a subset of the platform characteristic modes that realize the lowest AoA estimation error. Another recent breakthrough that exploits characteristic modes for AoA estimation is presented in [9], where Pöhlmann et. al discuss the potential of MIMO antennas for AoA estimation. The authors present a compact design obtained by exciting different sets of orthogonal characteristic modes on the same antenna element. Although modelling techniques are required to accurately represent the radiation pattern of the MIMO antenna, which may result in AoA estimation performance deterioration when separating multiple arriving signals or requirement of computationally expensive localization algorithms. The proposed system is a significant advance towards AoA estimation using compact devices.

In this article, we address the need for accurate and reliable AoA estimation using compact structures. As a fair benchmark, we use a state-of-the-art AoA estimation technique – MUltiple SIgnal Classification (MUSIC) algorithm [10], which is implemented the same way for all the arrays and antennas discussed in this work.

Methodology

To provide a fair and unbiased comparison between different antennas, the MUltiple SIgnal Classification (MUSIC) algorithm [10] is used in the proposed study. This is a state-of-the-art algorithm, which can be implemented with almost any multiport antenna, regardless of its configuration. It allows fair comparison between different set-ups. MUSIC is a search-based algorithm, centered on the eigen-decomposition of the received signals' covariance matrix. For more details about the algorithm, please refer to [3] and [11]. In this study, the AoA estimation performance is assessed in the following steps for each set-up concerned:

1) The far-field radiation patterns generated at each port of the MIMO antenna or antenna arrays are extracted from a full-wave electromagnetic simulator tool (CST Studio Suite). CST is a standard commercial software, used for antenna design and analysis. It was chosen as it offers accurate and efficient 3-D electromagnetic results, allowing optimization and fair comparison of different set-ups in an unbiased manner. The following assumptions are considered:
   - All the investigated configurations are simulated in the same CST setup solver.
   - For simplicity, the source signals and the antennas are assumed to be on the same horizontal plane, i.e. elevation plane fixed at $\theta = 90°$.
   - The AoA is then studied for the azimuth angles (horizontal plane) defined as ϕ_i with a resolution of $0.1°$.
2) The system signals are modelled in MATLAB:
   - White Gaussian noise is added for each signal incoming from ϕ_i directions. The noise is assumed to be spatially uncorrelated.
   - We assume that a total of K narrowband source signals with wavelength λ impinge on the antennas under test.
   - The algorithm assumes that $N > K$, i.e. the number of arriving signals is smaller than the number of antenna elements. This is a key assumption for multiple source separation in the MUSIC algorithm [3].
3) The MUSIC algorithm is implemented using the results of the covariance matrix obtained from the response of the antennas under test in step 2.
4) The estimated AoA is extracted as the peak value of the MUSIC spectrum function. The performance of the proposed AoA estimation algorithm is then evaluated in terms of Mean Absolute Error (MAE) between the MUSIC estimated angle and the actual incident angle.

Review of Antenna Arrays for AoA Estimation

Currently the most popular choice for performing AoA estimation is through antenna arrays. Array structures can be comprised of two types of antennas:

Directional antennas: these antennas radiate or receive electromagnetic waves more effectively in some directions than in others. They achieve increased performance in applications requiring more radiation in specific directions and allow suppression of interference from unwanted angles. Some examples of directional antennas are microstrip patch, horn, parabolic reflector and Yagi-Uda antennas.

Omnidirectional antennas: have a uniform pattern in one plane and a directional pattern in the orthogonal plane. A classic example of such pattern is the one generated by a dipole antenna.

Two of the most used array geometries for AoA estimation are:

Linear arrays: where the antennas are identical and placed in a straight line (see the schematic in Fig. 1). These struc-

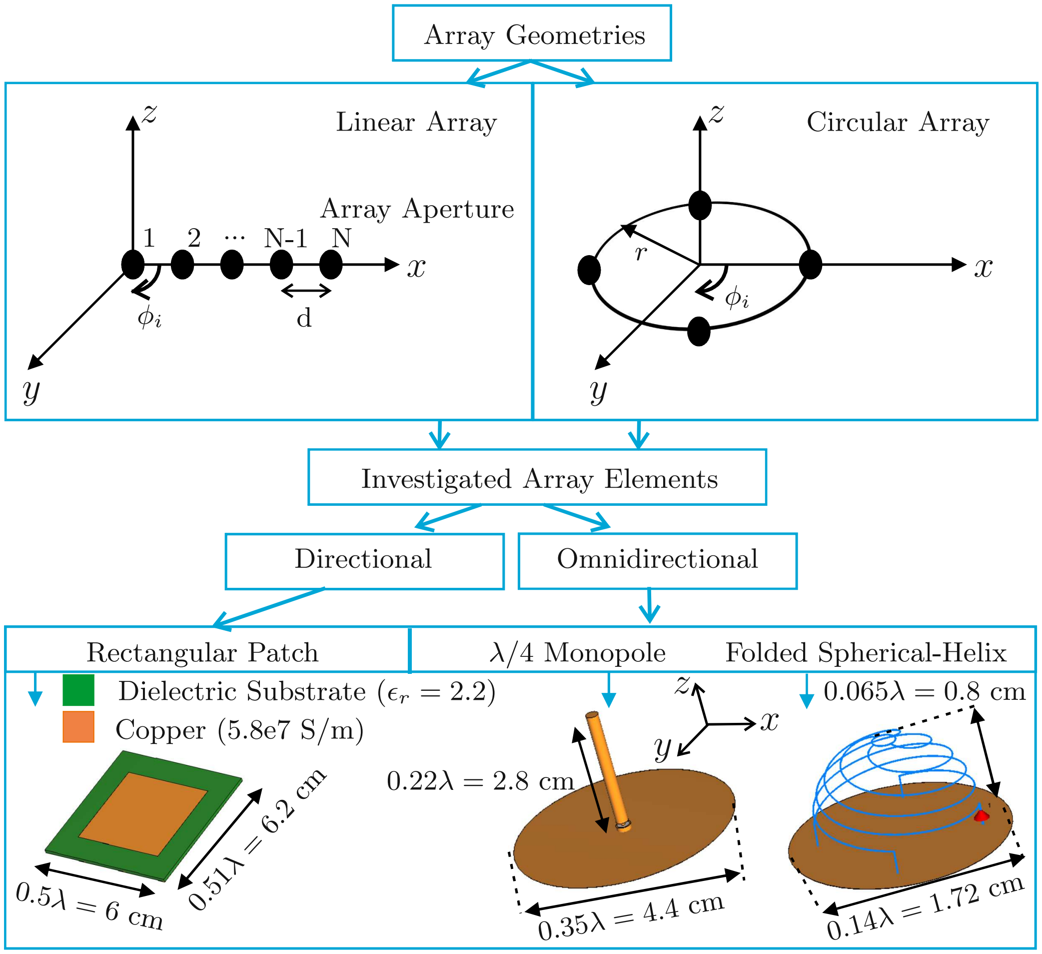

Fig. 1. Schematic summarizing the investigated antennas in this tutorial. The top part shows the most common array geometries used for AoA estimation: linear (top-left) and circular (top-right) arrays. Each of the proposed arrangement is then comprised of directional (rectangular patch) and omnidirectional ($\lambda/4$ monopole and folded helix antennas), the copper wires of the folded helix antenna are shown in blue for visualization. The corresponding dimensions of each element are given for the center operating frequency of 2.4 GHz. Note that because of the scalability of the investigated solutions, applications using higher/lower frequency will just require proportional scaling of proposed structures.

tures constitute the simplest array geometry and have been extensively investigated for AoA estimation [3], [4], [10], [12]. Linear arrays offer many advantages, such as easy manufacturing and availability of large number of signal processing algorithms.

For an incident signal incoming from angle ϕ_i, the distance between antennas will create a phase shift between elements proportional to the cosine of the angle. This means the signals at each direction will differ in phase, which is used for AoA estimation. Linear arrays using omnidirectional antennas face front-back ambiguity [3], [12], as the 'mirrored' signals incoming from two sides of the straight line containing the array elements will produce the same signal at antenna ports. While the use of directional antennas avoids this ambiguity, the linear array's field of view is still limited to $[0° - 180°]$. On top of that, the linear array's beamwidth is known to broaden near endfire directions. This practically limits the AoA estimation to a field of view of around $120°$ $[30° - 150°]$ [12]. Despite the aforementioned drawbacks (i.e., the need for an inter-element spacing of 0.5λ, and the beam broadening issue towards endfire directions), linear arrays are incorporated in many state-of-the-art off-the-shelf AoA estimation devices such as BOOSTXL-AOA SimpleLink™ Angle of Arrival BoosterPack and PDoA kit from Decawave [13]. Although those systems perform well in typical scenarios, the array size prevents their further miniaturization for size constrained IoT devices.

Circular arrays: where identical radiators are equally spaced on the circumference of a circle with radius r (as shown in the top-right corner of Fig. 1). Beyond a $360°$ view over the azimuth-plane, circular arrays also offer a consistent beamwidth over the azimuth-plane. If a suitable directional antenna is used, electronic beamsteering is obtained by simply shifting the excitation around the circular ring. This enables the circular array to have a more uniform beam pattern on the horizontal plane (xy-plane in Fig. 1). Contrary to linear arrays, circular arrays allow for a more constant AoA performance over the entire horizontal plane, i.e. $360°$ field of view. The AoA estimation performance of circular arrays comprised of omnidirectional and directional antennas has been discussed in [11]. The basic principle is the same as for a linear array: *the larger the distance between antennas, the greater the phase difference, and the better the resolution.*

TABLE I
COMPARISON OF COUPLING EFFECTS FOR LINEAR ARRAYS

S_{xy} (dB)	Inter-element spacing (d)		Half-power beamwidth		Coverage with MAE $< 1°$	
	$\lambda/4$ monopole	Folded helix	$\lambda/4$ monopole	Folded helix	$\lambda/4$ monopole	Folded helix
-13.5	0.5λ	0.5λ	$37.1°$	$37.2°$	$155°$	$155°$
-10	0.36λ	0.36λ	$47.7°$	$48.1°$	$146°$	$146°$
-8	0.28λ	0.3λ	$62°$	$63.3°$	$138°$	$141°$
-6	0.17λ	0.21λ	$112°$	$84.3°$	$109°$	$117°$

MINIATURIZATION OF ANTENNA ARRAYS

A common problem related to antenna arrays and their miniaturization is the electromagnetic interaction between individual antennas, known as mutual coupling. The presence of mutual coupling results in changes in the radiators' current distribution, leading to radiation of distorted beam patterns, change in antenna impedance, and reduced radiation efficiency [3]–[5].

The effects of mutual coupling in antenna arrays have been extensively treated in the literature, e.g. in [4]. It is generally agreed that mutual coupling is dependent on the spacing between the antennas, the type of antennas, and the method of excitation. Typically, for a relatively small number of antennas (as discussed in this article) a mutual coupling of $-10\,\text{dB}$ or lower has little effect on the overall antenna array performance [3], [4].

When the spacing between antennas is reduced, their mutual coupling increases. This becomes a significant source of errors in many AoA estimation algorithms that rely on the accurate knowledge of the received beam pattern [3]–[5], [10], [12]. Additionally, even when the mutual coupling level is known a priori, calibration techniques or correction procedures are needed to compensate for the mutual coupling effects. While the calibration methods may compensate for other mutual coupling effects, the gain deterioration of the antenna arrays is still a significant problem. To illustrate the effects of mutual coupling in AoA measurements, the methodology outlined in previous sections, is used to compare two omnidirectional linear antenna arrays composed of three elements. The first array is comprised of standard $\lambda/4$ monopole antenna, and the second – ultra-small folded spherical helix monopole with radius of 0.065λ designed by S. Best in [14]. Table I shows the element spacing required by each configuration to have the mutual coupling (S_{21} and S_{23}) of -13.5, -10, -8 and $-6\,\text{dB}$. Few conclusions can be drawn here:

First: as the element spacing is reduced, the mutual coupling between antennas increases and this translates into degradation in the AoA estimation performance. As shown in Fig. 2(a), the 0.5λ spacing yields lower Mean Absolute Errors (MAE) compared to smaller element spacing. The field of view with MAE smaller than $1°$ is detailed in Table I. For 0.5λ inter-element spacing ($-13.5\,\text{dB}$ coupling), both arrays have coverage of $155°$ $[12° - 167°]$. However, when the coupling level increases to $-6\,\text{dB}$, this coverage is reduced to around $109°$ $[36° - 145°]$ and $117°$ $[31° - 148°]$ for the $\lambda/4$ monopole and ultra-small folded helix, respectively. Note that, the $\lambda/4$ monopole array shows lower field of view (for -8 and $-6\,\text{dB}$)

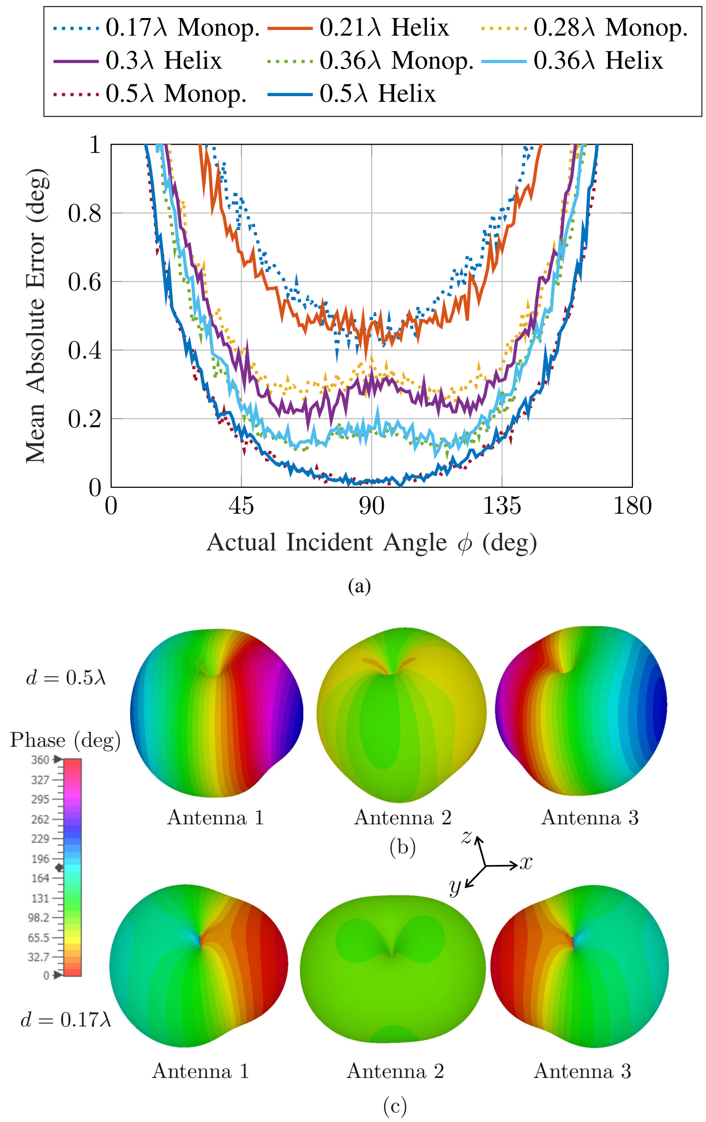

Fig. 2. Mutual coupling studies in 3-element linear arrays: (a) Comparison of MUSIC performance of $\lambda/4$ monopole and ultra-small folded helix antenna for different element spacing and $10\,\text{dB}$ SNR with 100 snapshots; (b) 3-D radiation patterns with color-coded phase of monopole antennas within linear array with 0.5λ inter-element spacing; (c) same radiation patterns with color-coded phase, but for an array with 0.17λ element spacing. Note that the patterns with spacing of 0.17λ exhibit smaller phase variation and their shape (amplitude) differs significantly from uniform omnidirectional pattern.

as the spacing between its elements is smaller than that of the ultra-small folded helix for similar level of coupling. The performance degradation in both arrays occurs due to the increased similarity of the phase of the radiation patterns [see Fig. 2(b) and Fig. 2(c)] and the beam broadening of the array pattern which increases from $37.1°$ to $112°$ for the $\lambda/4$ monopole and from $37.2°$ to $84.3°$ for the ultra-small folded helix (see Table I).

Second: the results demonstrate that as the element spacing is reduced, the mutual coupling for electrically small antennas (ultra-small folded spherical helix) degrades faster compared to the mutual coupling of the antennas not subjected to any miniaturization ($\lambda/4$ monopole). This is seen from Table I. For the array comprised of $\lambda/4$ monopoles, the element spacing can be reduced to 0.17λ for a $-6\,\mathrm{dB}$ coupling. However, the array using ultra-small folded spherical helix antenna cannot be reduced to less than 0.21λ for the same coupling level. *The implication is that the use of arrays comprised of highly miniaturized elements does not directly solve the problem of AoA estimation in compact devices, as the elements will experience increased mutual coupling when compared to designs not subjected to miniaturization.* It should be also noted that the effect occurs for very small inter-element spacing values, as for values greater than 0.36λ the effect is not noticeable.

Multimode MIMO Antennas

As an alternative to the classical arrays, we propose and advocate a new solution - multimode MIMO antennas. If properly designed, these antennas offer unprecedented size miniaturization while overcoming the above-mentioned issues with antenna coupling. Although MIMO antennas are used regularly to increase communication throughput using rich-multipath channels, this tutorial demonstrates they can be equally useful for AoA estimation.

The antenna studied here for AoA estimation applications is based on the design proposed in [15]. The key concept of this solution is that each port generates a radiation pattern with different radiating *modes*. The radiating *modes* need to show the following two properties:

1) omnidirectional radiation patterns [Fig. 3(b)].
2) orthogonal radiation patterns with different angular phase distribution in the horizontal plane [preferably with the phase changing linearly for uniform performance, see Fig. 3(b) and (c)].

For the proposed antenna [Fig. 3(a)], which employs 5 different *modes* fed through 5 ports, this principle is visualized in Fig. 3(c). Note, however, that theoretically an infinite number of modes and ports are feasible. It can be seen that port 1 has approximately constant phase over the entire horizontal plane, while for the *modes* generated in the middle part (ports 2 and 3) the phase changes twice in opposing directions, and finally for the bottom part (ports 4 and 5) the phase changes thrice, also in opposing directions. As with state-of-the-art antenna arrays, the phase of the multimode antenna is angle dependent [see Fig. 3(c)]. These phase-variations are used to determine the angle of the signal as it arrives to each antenna. However, while the classical array radiates a single mode and generates the required phase-variations through the inter-element spacing, the multimode design uses collocated antennas with no inter-spacing. In the absence of such inter-spacing, the phase-variations are obtained by forcing a rotation of the electric field in opposing directions around the antenna's perimeter, which generates phase-variations, depending on the number of turns of the phase for each radiated mode. The multimode principle allows AoA estimation from compact antennas, hence overcoming miniaturization limitations of classical antenna arrays. Furthermore, because the modes are – by definition – orthogonal, they provide a low correlation between the radiation patterns [15]. This results in small distortion of the radiation patterns, which is necessary to obtain accurate AoA measurements. The mutual coupling between the elements of the proposed antenna is therefore lower than $-14.9\,\mathrm{dB}$ at the center operating frequency. This concept offers a promising miniaturization solution for AoA-based localization when compared to current state-of-the-art off-the-shelf AoA estimation designs [13], as these models

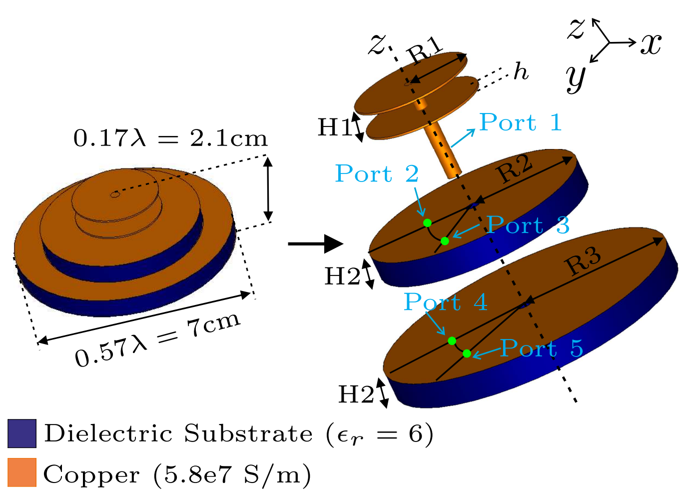

(a) Antenna dimensions: $h = 0.5\,\mathrm{mm}$, H1$= 8.7\,\mathrm{mm}$, H2$= 6.35\,\mathrm{mm}$, R1$= 14.2\,\mathrm{mm}$, R2$= 26.2\,\mathrm{mm}$, R3$= 36\,\mathrm{mm}$; Feed locations in mm (shown in green dots) Port $n = (x, y)$: Port 2 (-10.5,0), Port 3 = (-7.4,7.4), Port 4 = (-19,0), Port 5 = (-16.5,9.5).

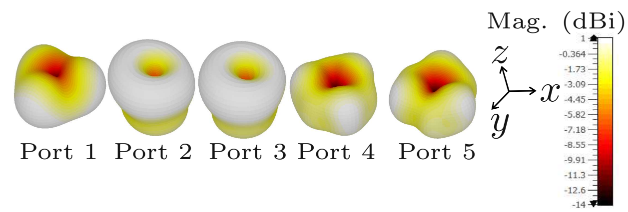

(b)

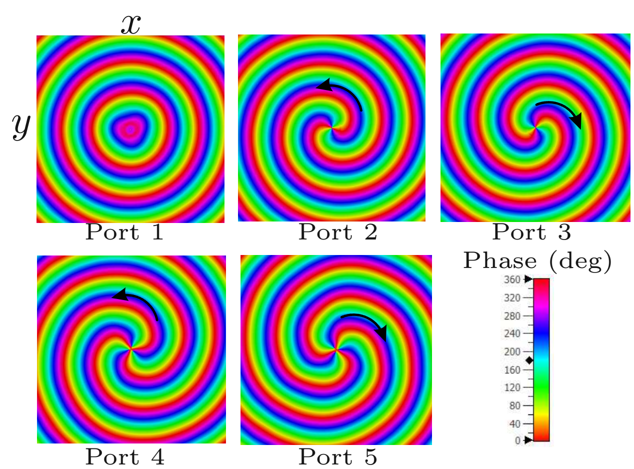

(c)

Fig. 3. Proposed antenna: (a) Perspective view showing the 3 collocated elements (left) and exploded view with marked ports (right); (b) 3-D amplitudes of the patterns of each *mode*, and (c) 2-D color-coded phase of the radiation patterns in $xy-$plane as it propagates outwards from the centrally located antenna.

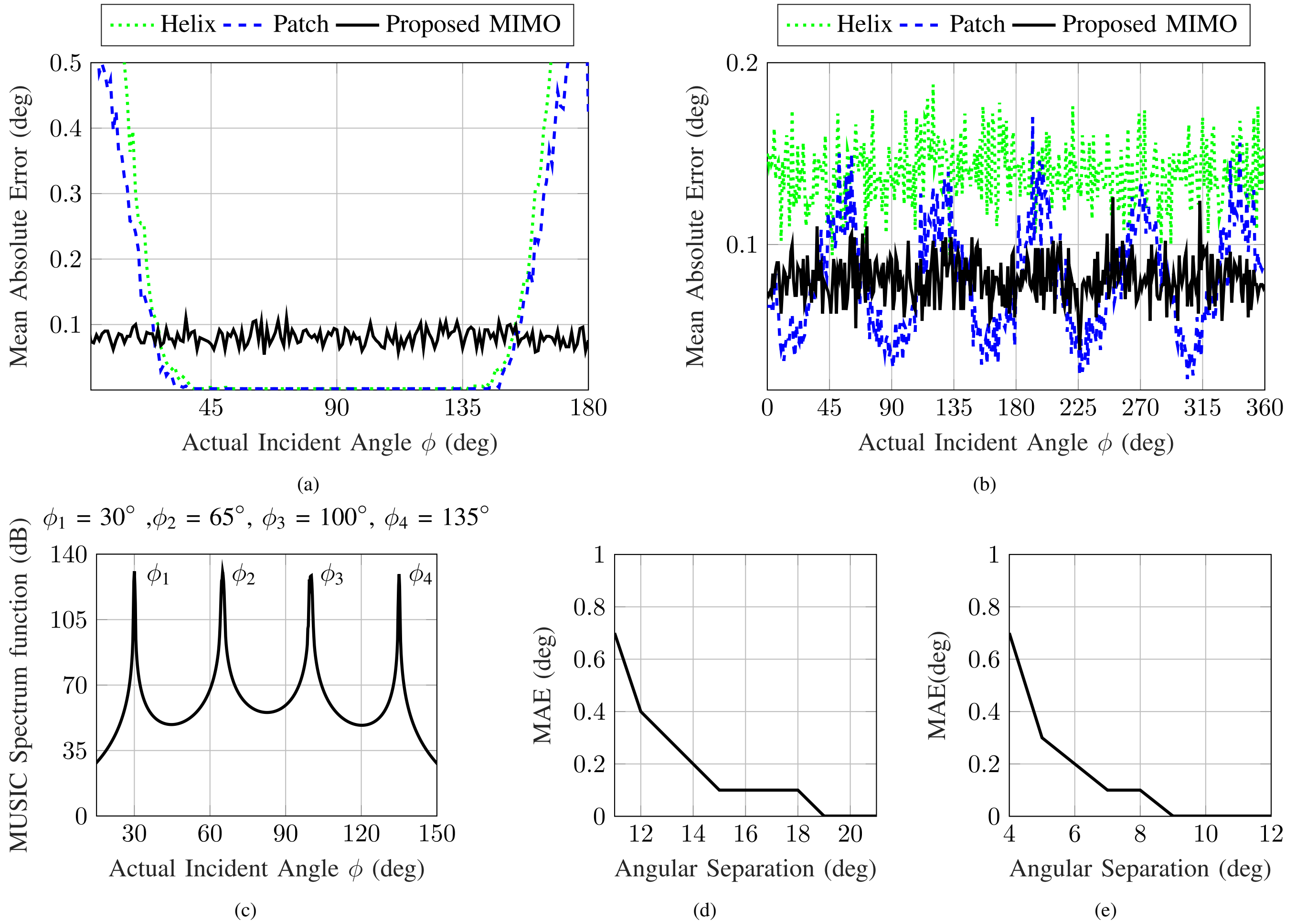

Fig. 4. Angle of arrival estimation performance of the investigated antennas: (a) Comparison between the proposed MIMO antenna and linear arrays; (b) Comparison between the MIMO antenna and circular arrays; (c) Four signals separation for the proposed MIMO antenna - using 200 snapshots and 10 dB SNR, for 35° angular separation; (d) Mean absolute error as a function of angular separation for three simultaneous arriving signals and (e) Mean absolute error as a function of angular separation for two simultaneous arriving signals.

still use antenna arrays with an inter-element spacing of 0.5λ.

ANGLE OF ARRIVAL PERFORMANCE

To investigate the AoA estimation performance of the proposed MIMO antenna, 5-element array structures comprised of antennas shown in previous sections are used for benchmarking. Those are directional patch antenna and omnidirectional ultra-small folded helix antenna. The spacing between antenna arrays is selected to allow the smallest possible separation that ensures a certain level of mutual coupling: unless stated otherwise, at least $10\,\mathrm{dB}$ of port-to-port isolation.

Single Signal Separation: Simulations were executed assuming $10\,\mathrm{dB}$ Signal-to-Noise-Ratio (SNR) level and each AoA measurement used 100 snapshots. Fig. 4(a) shows the mean absolute error (MAE) for the linear arrays and the 5-port MIMO antenna. The field of view with errors smaller than $0.11°$ is $132°$ $[24° - 156°]$ and $129°$ $[25° - 154°]$, respectively for the linear arrays comprised by the directional antenna (microstrip rectangular patch) and omnidirectional antenna (ultra-small folded spherical helix). It is seen that the 5-port MIMO antenna achieves an error smaller than $0.11°$ over the entire evaluated range. The MIMO antenna yields an error that does not change with direction, as opposed to linear arrays in which the estimated MAE increases near endfire directions. The proposed technique outperforms the linear arrays for angles smaller than $24°$ and greater than $156°$, offering an additional coverage of full plane. Even though the MIMO antenna is outperformed at broadside angles, it still achieves very low errors ($0.11°$). Most importantly, the compact structure has diameter = 0.57λ ($7.2\,\mathrm{cm}$, with zero inter-element spacing), compared to the linear arrays of length = 1.9λ ($23.7\,\mathrm{cm}$, inter-element spacing $= 0.44\lambda$, $-$ ultra-small folded spherical helix) and 2.26λ ($28.2\,\mathrm{cm}$, inter-element spacing $= 0.44\lambda$, $-$ rectangular patch). This means miniaturization by a factor of 3 to 4 or up to 75%.

As the proposed MIMO antenna offers $360°$ field of view, it can be compared with 5-element circular arrays [Fig. 4(b)]. The MIMO antenna achieves mean absolute errors smaller than $0.126°$ over the entire horizontal plane. The circular array comprised of directional patch achieves the lowest errors around $20°$, $92°$, $164°$, $236°$ and $308°$, as these angles fall in the broadside directions of the patch antenna orientation

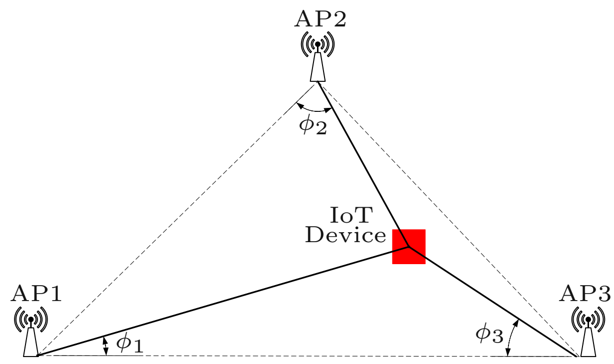

(a)

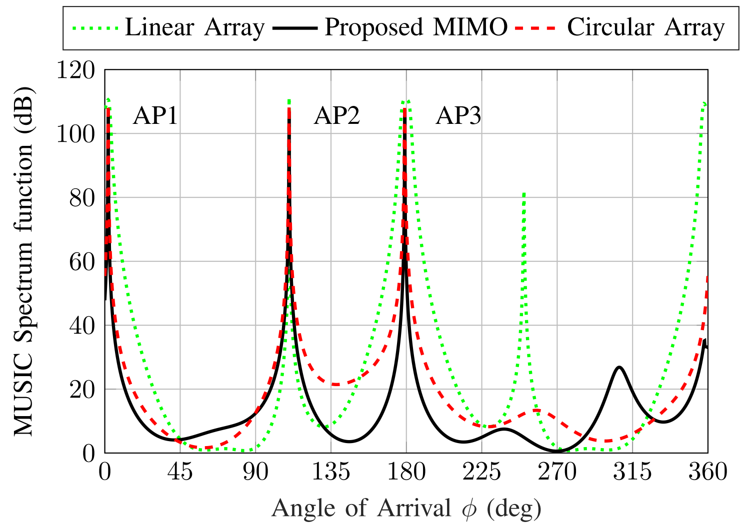

(b)

Fig. 5. Investigated IoT application case: (a) Line-of-sight scenario with three access points, and (b) Angle of Arrival estimation of the three access points (AP1 = $2°$, AP2 = $110°$, and AP3 = $179°$) using the proposed MIMO antenna, linear array and circular array.

in the circular array. Note that except for these directions, the MIMO antenna outperforms the patch antenna and the ultra-small folded helix antenna. The circular array of omnidirectional elements (ultra-small folded helix) shows the worst AoA performance, nevertheless the estimated MAE are still lower than $0.2°$ over the entire plane. These results present a very promising compact IoT solution for AoA-based localization, considering the size reduction obtained with the MIMO antenna (diameter = 0.57λ or $7.2\,\mathrm{cm}$), when compared to circular array comprised of rectangular patches (diameter = 0.93λ or $11.6\,\mathrm{cm}$, inter-element spacing of 0.43λ) and ultra-small folded spherical helix (diameter $= 0.94\lambda$ or $11.7\,\mathrm{cm}$, with inter-element spacing of 0.44λ). This translates to miniaturization of up to 40%.

Multiple Signals Separation: The number of signals that can be simultaneously separated in the MUSIC algorithm is limited to $N-1$, where N is the total number of antenna inputs. This means that for the proposed MIMO antenna a maximum of four simultaneous impinging signals can be analysed. However, the resolution of such separation does depend on antenna performance. To improve the accuracy of the system, due to the multiple signals impinging on the antennas, the simulations are conducted using 200 snapshots and $10\,\mathrm{dB}$ SNR. Fig. 4(c) shows the amplitude of the MUSIC spectrum for the proposed MIMO antenna when four signals with a $35°$ angular separation impinge on the antennas. The actual incident angles are: $\phi_1 = 30°$, $\phi_2 = 65°$, $\phi_3 = 100°$, and $\phi_4 = 135°$ and clear distinctive peaks are observed at those angles in the MUSIC spectrum function. To further illustrate the multiple signal performance of the proposed design, the peak MAE obtained from the MUSIC spectrum function and the actual incident angles for three and two simultaneous arriving signals were tested using different angular separations between those signals as shown in Fig. 4(d) and (e). When the number of signals is reduced, the capability to detect closely spaced signals is improved. For instance, for three and two signals the angular separation can be reduced to respectively $11°$ and $4°$. Overall, it can be seen that to separate three signals with peak MAE of $0.1°$, the angular separation needs to be at least $15°$, while a $7°$ angular separation achieves the same peak MAE of $0.1°$, for two simultaneous arriving signals.

IoT Application Scenario

To demonstrate the practical application of the proposed system within IoT framework, we investigated the problem of performing localization using size-constrained IoT platforms. Fig. 5(a) visualizes a potential IoT application that integrates the proposed multimode MIMO antenna. In the presented case a Line-of-Sight (LOS) scenario is assumed with three access points (APs). The APs which serve as localization anchors are located at (x, y) expressed in meters: AP1 at $(0, 0)$, AP2 at $(2.5, 4.3)$, and AP3 at $(5, 0)$; the angles of arrival are: $2°, 110°$, and $179°$. In the investigated scenario, the compact IoT device attempts of localize itself with respect to the APs. To perform triangulation, one needs to localize at least 3 signals, therefore an antenna with at least 4 ports is needed. Note that in this case the required signals to perform triangulation are detected simultaneously by using the MUSIC algorithm. Different approaches are studied in this tutorial: linear and circular arrays (using the smallest investigated antenna element, – the folded spherical helix antenna) or the proposed MIMO antenna. The MUSIC spectrum generated from 200 snapshots and $10\,\mathrm{dB}$ SNR is shown in Fig. 5(b). The results show that the linear array is capable of accurately detecting the angle of AP1 and AP2, while a $0.2°$ error is observed for the AP3. The $0.2°$ AoA estimation error results in a localization error of $13\,\mathrm{cm}$ when using the linear array system. Moreover, due to the linear array front-back ambiguity three additional target detections are seen at $180.2°$, $250.2°$, and $357.6°$. In contrast, the results using the circular array and the proposed MIMO show three clear peaks at the desired directions of the three APs, and the two systems are capable to accurately perform localization in the proposed scenario. Furthermore, as the arrays require dimensions of at least $23.2\,\mathrm{cm}$ (linear array) and $11.7\,\mathrm{cm}$ (circular array) to achieve the demonstrated AoA estimation and localization performances, such dimensions are challenging for small IoT devices. While the compact diameter of $7.2\,\mathrm{cm}$ needed by the proposed MIMO antenna, makes it suitable for small IoT packaging, e.g. IoT beacon technology used for access point identification in indoor navigation and tracking systems.

Conclusion

In this tutorial we gave an introduction to a new technique that allows high-performance AoA estimation from small IoT devices. Although the use of electrically small antennas is of increasing interest for AoA measurements, we pointed out some limitations to this approach. Moreover, we described the potentials of MIMO antennas for AoA applications. The proposed approach differs from classical antenna arrays, in that only the properties of the modes of collocated antennas (and not distance) are used for AoA estimation. This key practical feature offers a significant miniaturization capability for IoT devices. We demonstrated that by using the proposed method designers can achieve size reductions up to 75% and 40% when compared to linear and circular arrays, respectively. The presented work bridges the technical challenges of AoA estimation in compact IoT devices and high accuracy requirements. Thus, it has a very promising potential in guiding the design of future compact wireless localization systems.

Acknowledgment

This publication has emanated from research conducted with the financial support of Science Foundation Ireland under Grant number 18/SIRG/5612.

References

[1] J. Lin, W. Yu, N. Zhang, X. Yang, H. Zhang, and W. Zhao, "A Survey on Internet of Things: Architecture, Enabling Technologies, Security and Privacy, and Applications," *IEEE Internet Things J.*, vol. 4, no. 5, Oct. 2017, pp.1125–1142.

[2] F. Zafari, A. Gkelias and K. K. Leung, "A Survey of Indoor Localization Systems and Technologies," *IEEE Commun. Surveys, Tutorials*, vol. 21, no. 3, Apr. 2019, pp. 2568-2599.

[3] T. E. Tuncer and B. Friedlander, *Classical and Modern Direction-of-Arrival Estimation*, USA: Academic Press, Inc., 2009.

[4] M. G. Pralon, G. Del Galdo, M. Landmann, M. A. Hein and R. S. Thomä, "Suitability of Compact Antenna Arrays for Direction-of-Arrival Estimation," *IEEE Trans. Antennas Propag.*, vol. 65, no. 12, Dec. 2017, pp. 7244– 7256.

[5] B. Friedlander and A. Weiss, "Direction Dinding in the Presence of Mutual Coupling," *IEEE Trans. Antennas Propag.*, vol. 39, no. 3, Mar. 1991, pp. 273–284.

[6] C. Sun, H. Harada, and N. C. Karmakar, "Direction of Arrival Estimation Based on a Single-Port Smart Antenna for RFID Applications," John Wiley & Sons, Ltd., 2010, ch. 12, pp. 317–340.

[7] C. Y. Kataria, G. X. Gao, and J. T. Bernhard, "Design of a Compact Hemispiral GPS Antenna With Direction Finding Capabilities," *IEEE Trans. Antennas Propag.*, vol. 67, no. 5, Feb. 2019, pp. 2878–2885.

[8] R. Ma and N. Behdad, "Design of Platform-Based HF Direction-Finding Antennas Using the Characteristic Mode Theory," *IEEE Trans. Antennas Propag.*, vol. 67, no. 3, Mar. 2019, pp. 1417–1427.

[9] R. Pöhlmann, S. A. Almasri, S. Zhang, T. Jost, A. Dammann, and P. Hoeher, "On the Potential of Multi-Mode Aantennas for Direction-of-Arrival Estimation," *IEEE Trans. Antennas Propag.*, vol. 67, no. 5, May 2019, pp. 3374–3386.

[10] R. Schmidt, "Multiple Emitter Location and Signal Parameter Estimation," *IEEE Trans. Antennas Propag.*, vol. 34, no. 3, Mar. 1986, pp. 276–280.

[11] B. R. Jackson, S. Rajan, B. J. Liao, and S. Wang,"Direction of Arrival Estimation Using Directive Antennas in Uniform Circular Arrays," *IEEE Trans. Antennas Propag.*, vol. 63, no. 2, Feb. 2015, pp. 736–747.

[12] P. Ioannides and C. Balanis, "Uniform Circular Arrays for Smart Antennas," *IEEE Antennas Propag. Mag.*, vol. 47, no. 4, Aug. 2005, pp. 192–206.

[13] I. Dotlic, A. Connell, H. Ma, J. Clancy, and M. McLaughlin, "Angle of Arrival Estimation Using Decawave DW1000 Integrated Circuits," Proc. Workshop Positioning, Navigation and Commun., Oct. 2017, pp. 1–6.

[14] S. Best,"The Radiation Properties of Electrically Small Folded Spherical Helix Antennas," *IEEE Trans. Antennas Propag.*, vol. 52, no. 4, Apr. 2004, pp. 953– 960.

[15] A. Zandamela, K. Schraml, S. Chalermwisutkul, D. Heberling and A. Narbudowic, "Digital pattern synthesis with a compact MIMO antenna of half-wavelength diameter," *AEÜ – Int. J. Electron. Commun.*, vol. 135, Jun. 2021, pp. 153728.